Journal of Catalysis 258 (2008) 199–209

Contents lists available at ScienceDirect

Journal of Catalysis

www.elsevier.com/locate/jcat

Deoxygenation of methylesters over CsNaX

Tawan Sooknoi [1], Tanate Danuthai [2], Lance L. Lobban, Richard G. Mallinson, Daniel E. Resasco *

School of Chemical, Biological and Materials Engineering, University of Oklahoma, Norman, OK 73019, USA

ARTICLE INFO

Article history:
Received 15 April 2008
Revised 4 June 2008
Accepted 8 June 2008
Available online 18 July 2008

Keywords:
Basic zeolites
CsNaX
Biofuels
Methylesters
Deoxygenation
Decarbonylation
Deacetalation
Hydrogenation
TPD
TPRx

ABSTRACT

The deoxygenation of methyl octanoate over a CsNaX zeolite catalyst has been investigated as a model reaction for the production of de-oxygenated liquid hydrocarbons from biodiesel. Several operating parameters were investigated, such as the type of basic catalyst used, the co-reactant incorporated in the reactor as a solvent of the liquid feed, and the reaction temperature. The CsNaX zeolite used in the study was prepared by ion exchange of NaX with $CsNO_3$/CsOH solution. A significant role of the solvent (co-reactant) was found on the activity, selectivity, and stability of the catalyst. That is, when methanol was co-fed enhanced stability and decarbonylation activity were observed. By contrast, when nonane was used, the catalyst deactivated rapidly and the selectivity to coupling products was enhanced. Temperature programmed desorption (TPD) of methyl octanoate and methanol, as well as flow catalytic studies suggest that methyl octanoate first decomposes to an octanoate-like species. The decomposition of such species leads to the formation of heptenes and hexenes as major products. Octenes and other hydrogenated products are formed in lower amounts via hydrogenation by hydrogen produced on the surface by methanol decomposition, but not from gas phase H_2, followed by dehydration. When the polarizable Cs cation is not present in the catalyst, reduced activity and formation of undesired products, such as aromatics and pentadecanone, occur. Similarly, non-zeolitic basic catalysts, such as MgO, exhibit low activity and low selectivity to de-oxygenated liquid hydrocarbons.

© 2008 Elsevier Inc. All rights reserved.

1. Introduction

The interest in renewable fuels as replacements for fossil fuels has rapidly increased over the past few years. Among the various fuels-from-biomass investigated, fatty acid methyl-ester biofuels (FAME) obtained by trans-esterification of triglycerides from natural oils and fats with methanol have received considerable attention [1–4]. They exhibit high cetane number and are considered to burn cleanly; however, there is growing concern about the fungibility of these fuels with conventional petroleum-derived diesel due to the oxidative and thermal instability [5–7]. Reduction of the oxygen content in the fuel would readily improve the stability of the fuel and therefore its utilization potential. Various processes including hydrogenolysis [8,9], decarbonylation [10,11], and decarboxylation [12,13] of FAME have been proposed to transform the biodiesel into the hydrocarbon base fuel.

The decarbonylation and decarboxylation have advantages over hydrogenolysis because, while the hydrocarbons thus produced may contain less carbon than its fatty acid counterpart, the former reactions require much less hydrogen than the latter [8]. Moreover, the properties of the fuel obtained by decarbonylation/decarboxylation are not significantly different from those obtained from hydrogenolysis [12]. Typically, decarbonylation takes place over supported noble metal catalysts at relatively high temperature (>350 °C) [14]. For example, Pd/C has been found to be an effective catalyst for decarbonylation/decarboxylation [12]. However, CO produced from the reaction may competitively adsorb on the metal surface, leading to a reduction or even loss in the catalytic activity as conversion increases. Hence, the required total and hydrogen partial pressures are generally high, in order to keep the surface clean and facilitate the oxygenate–metal surface interaction, while reducing catalyst deactivation [15].

An alternative family of catalysts that may overcome some of these limitations is that of solid bases. This is because the FAME is fairly electrophilic while the decarbonylated by-product, CO, is nucleophilic. Thus, while the adsorption of FAME over basic catalyst may be strong and the reaction can be readily promoted at atmospheric pressure, the by-product CO should promptly leave the basic surface. As a result, considerably lower temperature and hydrogen partial pressure may be required. Among possible solid base catalysts, low-silica zeolites containing highly polarizable cations, such as cesium, may be good candidates. These catalysts have been found to exhibit relatively high activity towards reactions involving oxygenates [16,17], as well as hydrogenation and hydrogenolysis of

* Corresponding author. Fax: +1 (405) 325 5813.
E-mail address: resasco@ou.edu (D.E. Resasco).
[1] Permanent address: Department of Chemistry, Faculty of Science, King Mongkut's Institute of Technology, Ladkrabang, Bangkok 10520, Thailand.
[2] Permanent address: Petroleum and Petrochemical College, Chulalongkorn University, Patumwan, Bangkok 10330, Thailand.

0021-9517/$ – see front matter © 2008 Elsevier Inc. All rights reserved.
doi:10.1016/j.jcat.2008.06.012

acrylonitrile and propionitrile [18]. It has been suggested that, in addition to the need for strong basicity, an active catalyst requires the co-existence of acid and basic sites for reactions such as hydrogenation and hydrogenolysis [19]. In fact, an alkali-exchanged zeolite such as the CsNaX contains conjugate acid–base pairs, in which the exchangeable alkali cation has Lewis acidity and the oxygen that bridges Si and Al near the exchangeable cation has basicity [20].

The purpose of this work is to investigate deoxygenation reactions on Cs and NaX zeolite catalysts using methyl octanoate as a model feed that may mimic some of the most relevant reactions involved in the refining of biodiesels. The effects of varying reaction conditions such as temperature, hydrogen partial pressure, feed concentration, presence of competing molecules, as well as catalyst formulations were investigated in a flow reactor. In addition, temperature programmed techniques were employed to elucidate possible reaction pathways thought to be relevant in the deoxygenation of FAME.

2. Experimental

2.1. Catalyst preparation and characterization

Commercial molecular sieve (UOP type 13X, NaX) and MgO (LOT No. 130337) were obtained from Fluka and Schweizerhall, respectively. The as-received materials were calcined at 450 and 700 °C, respectively. The Cs-containing zeolite (CsNaX) was prepared by ion exchange of molecular sieve 13X with 0.1 M $CsNO_3$/CsOH (4/1 v/v) at 80 °C for 24 h. The solid material was filtered and left to dry at 80 °C overnight. The sample was then calcined at 450 °C for 2 h in a flow of dry air. It has been demonstrated that crystallinity in CsNaX samples is largely retained after this treatment [21]. To investigate the effect of excess Cs in the zeolite, the CsNaX sample was washed repeatedly with water, a treatment that eliminated a significant fraction of Cs.

Surface areas of the CsNaX, before and after washing, and NaX catalysts were determined by nitrogen adsorption at 77 K using a Micromeritics ASAP 2000 apparatus. X-ray diffraction (XRD, Bruker AXS D8Discover) was employed to investigate the catalyst structure. The hydrogen uptake of the catalysts was measured by temperature programmed reduction (TPR) in an apparatus constructed for this purpose.

2.2. Temperature-programmed desorption (TPD) of isopropylamine

The catalyst acidity was tested by the amine TPD technique. First, 50 mg of sample was pretreated at 450 °C in a flow of 2% O_2/He for 1 h. After the pretreatment, the sample was cooled in He to room temperature and then consecutive 10 µl pulses of isopropylamine (IPA) were injected to the sample until saturation was achieved, as indicated by a constant $m/z = 44$ signal in the MS. After removing the excess IPA by flowing He for 3 h, the sample was linearly heated to 700 °C at a heating rate of 10 °C/min. Masses (m/z) of 44, 41, and 17 were monitored to determine the evolution of desorbing species and MS fragments. The signal 44 is only due to IPA; by contrast, 41 and 17 are due to propylene and ammonia, respectively, but also to MS fragments of IPA. To determine whether there is desorption or decomposition, one follows the evolution of the three signals simultaneously. In this case, no decomposition was observed and the three signals kept the same ratio throughout the desorption. The amount of desorbed IPA was calibrated with 50 µl pulses of 2% propylene in He ($m/z = 41$).

2.3. Temperature-programmed desorption (TPD) of methyl octanoate

The evolution of pre-adsorbed methyl octanoate over CsNaX catalysts was followed by TPD. In each run, 50 mg of the sample was initially pretreated in a flow of 2% O_2/He for 2 h at 450 °C. Then, the sample was cooled in He flow to 150 °C. A 100 µl pulse of methyl octanoate was injected to the sample, and a He flow was introduced for 3 h at 150 °C in order to remove the excess methyl octanoate. The sample was then heated to 900 °C at a rate of 10 °C/min. Masses (m/z) of 2, 28, 56, and 74 were monitored to determine the evolution of hydrogen, carbon monoxide, hydrocarbons, and methyl octanoate, respectively.

2.4. Temperature-programmed desorption (TPD) and temperature programmed reaction (TPRx) of methanol

Methanol was chosen as a probe for the zeolite surface and as a co-reactant to help reduce the rate of catalyst deactivation during the conversion of methyl octanoate. Therefore, the desorption and decomposition of methanol over CsNaX and NaX catalysts were investigated by TPD and TPRx techniques in the same apparatus described in the previous section. In each run, 50 mg of the sample was initially pretreated in a flow of 2% O_2/He for 2 h at 450 °C. Then, the sample was cooled in He flow to room temperature. In the desorption experiment, 10 µl of methanol was repeatedly injected over the sample at room temperature until reaching saturation, as indicated by a steady MS signal. After removal of the excess methanol by flowing He for 3 h at room temperature, the sample was heated to 900 °C at a rate of 10 °C/min. For the TPRx experiment, methanol was continuously fed through the sample bed at a flow rate of 1 ml/h. The sample was linearly heated from room temperature to 700 °C at a heating rate of 10 °C/min. Masses (m/z) of 2, 28, 31, and 45 were monitored to determine the evolution of hydrogen, carbon monoxide, methanol, and dimethylether, respectively.

2.5. Catalytic activity measurements for the deoxygenation of methyl octanoate

The deoxygenation of methyloctanoate was carried out at atmospheric pressure, in a fixed bed flow reactor made with 1/4″ quartz tube. Prior to the reaction, the catalyst samples were pretreated in situ under flow of 2% O_2/He at 450 °C for 2 h. Then, the catalyst bed was cooled to the reaction temperature (425 °C) under flow of He (25 ml/min). The reactant feed of 10 wt% methyl octanoate in methanol solvent was introduced into the reactor using a syringe pump via a heated vaporization port. Alternatively, in some runs, nonane was used as a solvent instead of methanol. Unreacted feed and products were quantified using an online GC-FID equipped with a capillary HP-5 column, following a temperature program to optimize product separation.

2.6. Temperature-programmed oxidation (TPO) of coke deposits after reaction

Temperature-programmed oxidation (TPO) was employed to investigate and quantify the nature and amount of coke deposited on the spent catalysts. 30 mg of the sample was packed in the 1/4″ quartz tube reactor. The temperature was ramped to 900 °C with a heating rate of 10 °C/min and the TPO profiles were recorded under flow of 2% O_2/He. The CO_2 produced by the oxidation of the coke deposits was further converted to methane over a methanation catalyst (15% Ni/Al_2O_3) in the presence of hydrogen at 400 °C. The corresponding methane was then analyzed online by an FID detector. The amount of oxidized coke was calibrated using 100 µl pulses of pure CO_2 injected to the same system.

Table 1
Elemental analysis data of NaX and CsNaX catalysts

Catalysts	Surface area (m^2/g)	Total composition	
		Si/Al	Cs/Al
NaX	745	1.2	–
Washed CsNaX	506	1.2	0.47
CsNaX	468	1.2	0.62

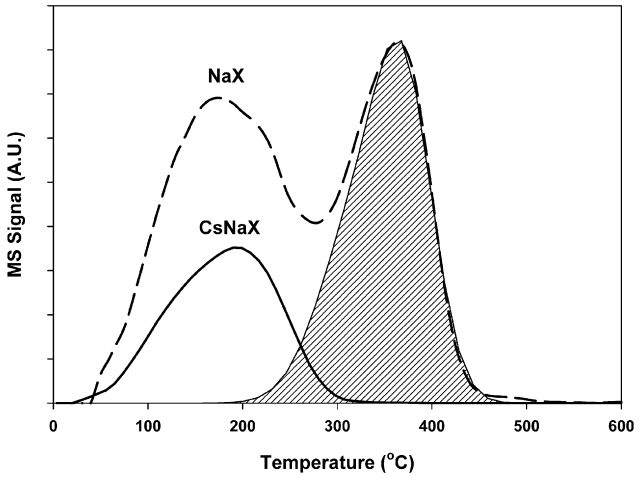

Fig. 1. Evolution of $m/z = 44$ during TPD of isopropylamine.

3. Results

3.1. Characterization of the fresh catalysts

The NaX and CsNaX catalysts were characterized by XRD and BET surface area analysis. The XRD pattern of CsNaX catalyst showed almost the same pattern as that of NaX, which confirms that the CsNaX catalyst contains practically the same crystalline phase after the cesium exchange. The atomic bulk (ICP) compositions of NaX and CsNaX catalysts are presented in Table 1. The analysis indicates that a significant fraction of the initial Na ions have been exchanged by Cs. This significant amount of ion exchange plus some excess Cs occluded in the zeolite resulted in a noticeable drop in BET surface area and pore volume, as compared to those of the original NaX. This is because the Cs cation is much larger than the Na cation and the exchange leads to a reduction of the available pore volume and surface area. This observation is in good agreement with previous reports [22,23]. However, it must be noted that, as the CsNaX sample was dried without washing during the preparation, excess Cs cations were left on the sample as bulk particles of cesium oxide, cesium carbonate, cesium peroxide, or cesium superoxide. Therefore, a fraction of the observed drop in BET may be due to pore blockage by these species. The washing treatment eliminated part of this Cs and resulted in a partial recovery of the BET area.

The TPD of isopropylamine suggested that alkali-exchanged zeolite possesses some acidity. As shown in Fig. 1, the evolution of adsorbed IPA at lower temperature (∼180 °C) corresponds to the weak adsorption of IPA on the zeolite framework, while that at higher temperature may represent acid sites, but not the strong Brønsted sites typically found in HY or HZSM-5. In those cases, the IPA does not desorb at high temperatures as a whole molecule, but rather it decomposes into propylene and ammonia. In the present zeolites, there is no decomposition, but rather desorption. Quantification of the desorbed amount resulted in about 2.9 $\mu mol/g_{cat}$ for the weakly adsorbed IPA on CsNaX catalyst, but no strongly adsorbed species. By contrast, on the NaX zeolite, about 4.6 $\mu mol/g_{cat}$ were weakly adsorbed and 3.6 $\mu mol/g_{cat}$ strongly adsorbed, which

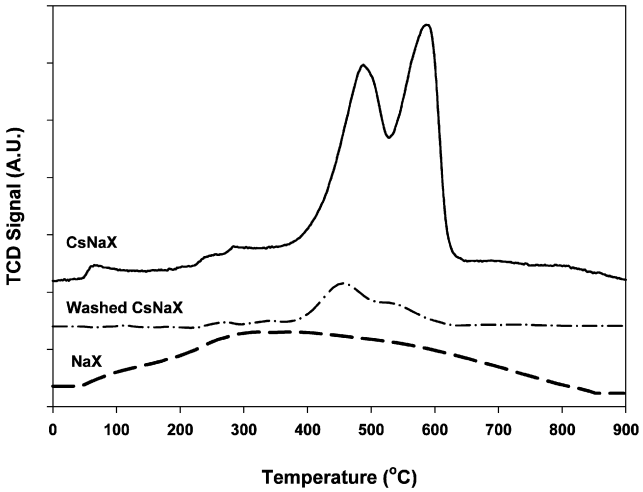

Fig. 2. TPR of CsNaX (before and after washing) and NaX catalyst; all of them treated in air at 450 °C before starting the TPR.

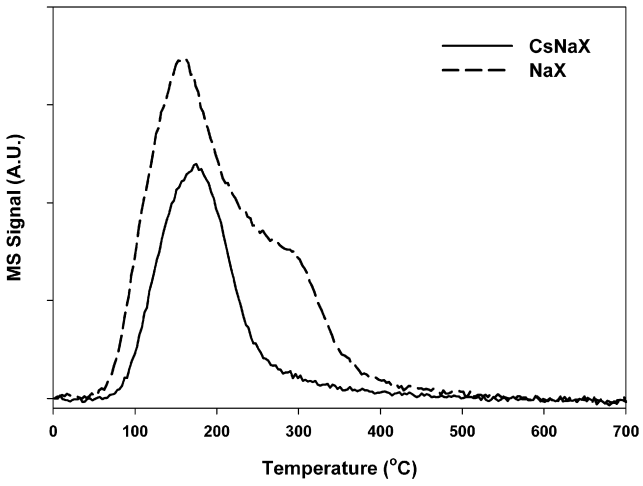

Fig. 3. TPD profiles of adsorbed methanol over CsNaX and NaX catalysts.

is consistent with the presence of some residual acidity on this catalyst.

The hydrogen consumption of the two fresh zeolites catalysts was quantified by the temperature programmed reduction (TPR) technique. As shown in Fig. 2, a significant amount of hydrogen consumption can be observed at around 550 °C over the CsNaX zeolites whilst no hydrogen was consumed by the NaX sample. Relatively less hydrogen consumption can be observed as successive washing steps were applied to the CsNaX sample. Therefore, it is clear that the high hydrogen consumption observed on the unwashed CsNaX is due to the reduction of the excess cesium species [24,25]. The Cs bulk species (oxides or carbonates) may be formed from excess Cs during the activation in air. The hydrogen consumption increases with the amount of excess cesium species in the sample.

3.2. Temperature-programmed desorption (TPD) and reaction (TPRx) of methanol

The evolution profiles obtained from TPD of adsorbed methanol are shown in Fig. 3. A significantly higher amount of undissociated methanol is desorbed from the NaX catalyst than from CsNaX. Moreover, while the NaX zeolite exhibited two desorption peaks at temperatures around 150 and 300 °C, the CsNaX zeolite only displayed the lower-temperature peak. Similar differences in the TPD

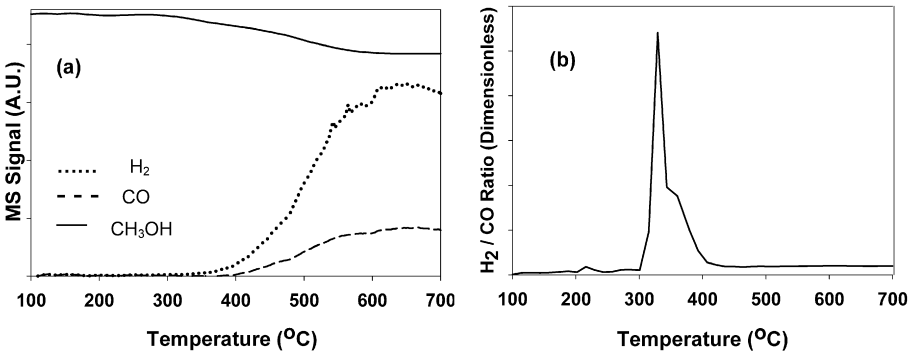

Fig. 4. (a) Temperature-programmed reaction of continuous flow methanol over CsNaX. (b) H_2/CO signal of continuous flow methanol over CsNaX.

profiles of adsorbed methanol on NaX and CsNaX have been previously observed [26]. These differences were suggested to arise from a stronger interaction of the adsorbate with the Na cations in NaX, as compared to those in CsNaX. However, other adsorption studies [27,28] would indicate that one could also assign the lower temperature TPD peak to methanol adsorption on sites located in the supercages of the NaX and the higher temperature peak to sites located in the smaller sodalite cages. The difference in binding strength in the two sites can be explained in terms of the shorter-range interactions taking place in the small cavities of the sodalite cages. Accordingly, the disappearance of the high temperature peak from the TPD of the CsNaX indicates that the presence of the much larger Cs cations in the small sodalite cage dramatically reduces its accessible pore volume, thus preventing the adsorption of methanol on these sites. Based on this description, adsorption on the CsNaX zeolite would occur only in the larger supercages, but even this peak is smaller than the corresponding one on NaX, due to the larger extent of blocking by Cs.

To investigate the temperature range that is more relevant to the reaction studies, the decomposition of methanol over CsNaX was examined by temperature programmed reaction (TPRx) under continuous flow of methanol. As shown in Fig. 4a, the decomposition of methanol starts at 300 °C, and in agreement with previous studies [29], hydrogen (H_2), and carbon monoxide (CO) are the main decomposition products. However, it is interesting to note that they do not appear at the same time. To make this trend more clearly visible, the H_2/CO ratio is plotted in Fig. 4b. A sharp rise in this ratio is observed above 300 °C, but it goes back to a constant low value at higher temperatures. This observation suggests that methanol primarily decomposes into H_2 that desorbs and a fragment that remains on the surface. The species retained on the surface has been previously identified by ^{13}C NMR [30] and suggested to be a formate-like species. As the temperature is increased, this formate-like species can further decompose evolving CO. Beyond this temperature the continuous decomposition produces both CO and H_2.

The desorption characteristics of methyl octanoate over CsNaX catalyst are shown in Fig. 5. Unlike the case of methanol, the TPD of adsorbed methyl octanoate reveals no evolution of the parent methyl octanoate molecule, suggesting that this is strongly adsorbed. Instead, decomposition products are observed. CO and H_2 were initially evolved above 300 and 400 °C, respectively. From the areas, we have quantified the amount of CO evolved below 450 °C to be about 1.6 μmol/g_{cat}. This amount of CO is produced by the decomposition of methyl octanoate at the methoxyl group. On the other hand, a larger amount, 6.8 μmol/g_{cat} of CO, is produced at temperatures higher than 450 °C from the decarbonylation of methyl octanoate. It is important to note that, contrary to methanol, essentially no hydrogen is evolved up to about 400 °C. A significant amount of hydrogen (4 μmol/g_{cat}) was only produced at ~450 °C.

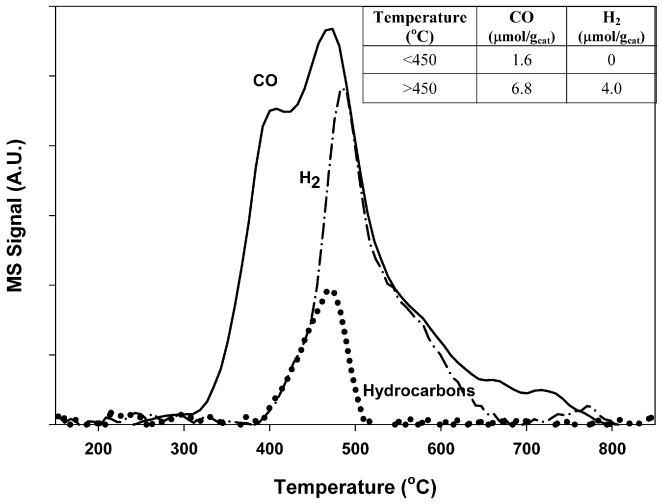

Fig. 5. TPD profile of adsorbed methyl octanoate on CsNaX zeolite catalyst.

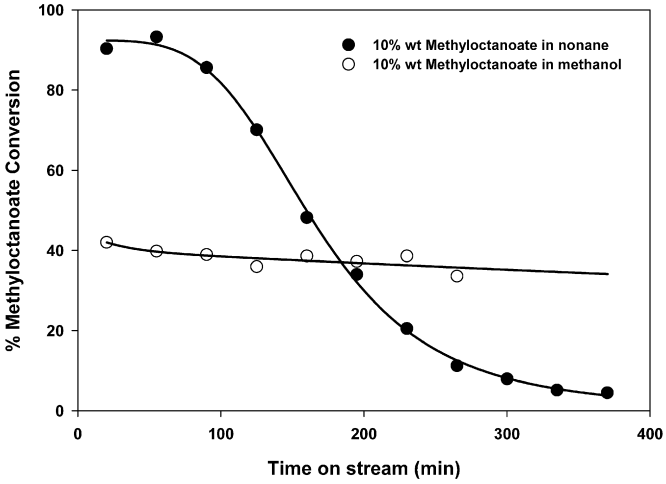

Fig. 6. Conversion of 10 wt% methyl octanoate over CsNaX using nonane and methanol as solvent as a function of time on stream. Reaction conditions: 425 °C, 1 atm, $W/F = 198$ g h/mol, 25 ml/min of He.

3.3. Reaction under continuous flow of methyl octanoate

3.3.1. CsNaX catalyst

The effect of co-feeding methanol was investigated during the decarbonylation of methyl octanoate over the basic CsNaX zeolite catalyst. The conversion obtained by using either nonane or methanol as a solvent is compared in Fig. 6. It can be seen that when nonane was used, a high activity was observed at the be-

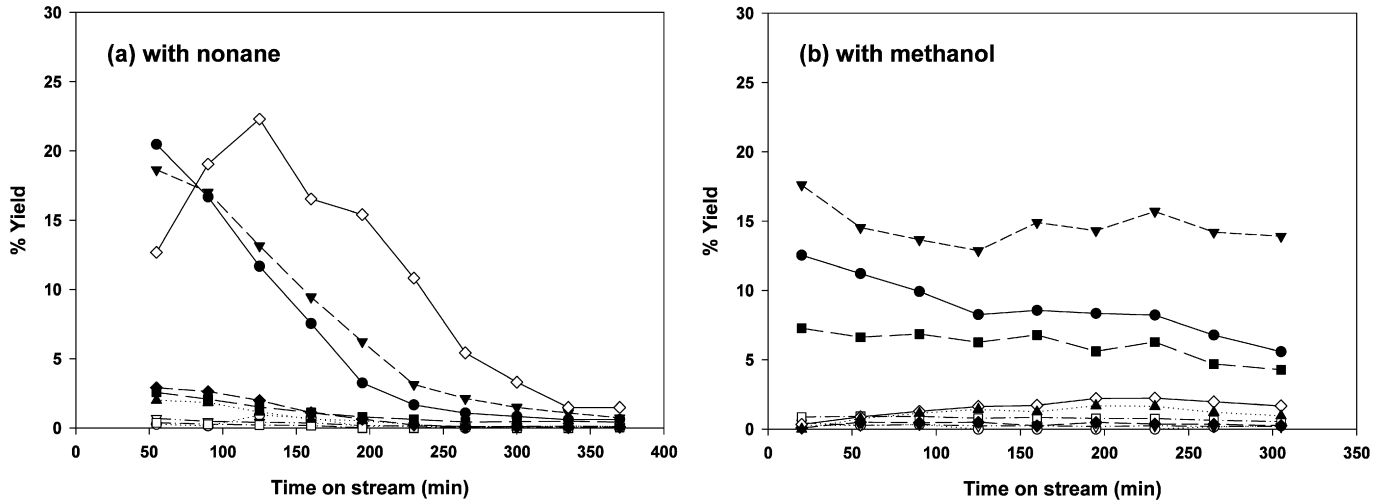

Fig. 7. Product distribution from the reaction of 10 wt% methyl octanoate using (a) nonane and (b) methanol as solvent as a function of time on stream. Reaction conditions: 425 °C, 1 atm, $W/F = 198$ g h/mol, 25 ml/min of He. Heptenes (▼), hexenes (●), octenes (■), pentadecanone (◇), coupling ester (▲), octane (□), tetradecene (◆), heptane (▽), hexane (○).

Table 2
Product distribution from reaction of 10 wt% methyl octanoate in methanol over CsNaX at various space time

	W/F (g h/mol)		
	99	198	396
Conversion	24.0	37.2	62.3
Yield (%)			
Hexenes	4.5	8.8	19.3
n-Hexane	0.2	0.1	0.3
Heptenes	8.9	14.6	26.1
n-Heptane	0.1	0.2	0.8
Octenes	3.0	6.1	6.7
n-Octane	0.4	0.8	1.0
Octanal	0.6	0.5	0.4
Oxygenates	1.9	2.0	3.3
Octanonic acid	0.8	1.1	2.2
Tetradecene	0.3	0.3	0.6
Pentadecanone	2.0	1.5	0.9
Coupling ester	1.2	1.1	0.8

Reaction conditions: 425 °C, 1 atm, 25 ml/min of He.

ginning of the reaction; however, this activity was rapidly lost by catalyst deactivation. On the other hand, while a relatively lower activity was observed when methanol was cofed into the reaction system, a much better stability with time on stream was obtained.

The product distributions from the decarbonylation of 10 wt% methyl octanoate over CsNaX using nonane and methanol as solvents are compared in Figs. 7a and 7b, respectively. In the reaction co-feeding nonane, the dominant product was 8-pentadecanone, a coupling product of methyl octanoate. Deoxygenated products, namely octene, heptene and hexane were also observed, but with lower selectivities. When methanol was used as a solvent, very small amounts of coupling products (i.e. 8-pentadecanone) were obtained. In this case, the reaction products were mostly heptenes, hexenes, and octenes; that is, the dominant reactions were decarbonylation (elimination of CO), deacetalation (elimination of CH_3CHO), and hydrogenation/dehydration (elimination of O). It is clear that while the conversion of methanol itself is rather low (∼5%), its presence greatly affects the product distribution and stability of the catalyst.

Table 2 summarizes the product distribution from the reaction of 10 wt% methyl octanoate in methanol at various space times (W/F). As discussed above, the major product is C7 hydrocarbons (i.e. heptenes), which is the expected product from direct decarbonylation of methyl octanoate over CsNaX. In addition, significant amounts of hexene are obtained. As discussed below, we believe that hexenes are products of deacetalation. In significantly lower concentrations, octenes and coupling products, together with small amounts of octanes and oxygenates, were also observed. As shown in Figs. 8a and 8b, the yields of heptenes and hexenes increase parallel to the overall conversion as a function of W/F, suggesting that both are primary products. That is, hexene is not a secondary product arising from the cracking of heptene. By contrast, as shown in Fig. 8b, the evolution of octene follows a different pattern; it seems to reach a plateau at an overall conversion near 40% and the start of this plateau coincides with the increase in the formation of secondary products such as lower oxygenates, octanoic acid, and tetradecene (see Fig. 8c). On the other hand, the coupling products exhibit a drop in the concentration as a function of W/F, indicating that these heavier compounds tend to react further into lighter compounds as the catalyst bed increases.

A major consideration in the production of fuels from biomass is the consumption of hydrogen [31], which is typically needed in reactions involving deoxygenation steps. We have investigated the impact of the presence of hydrogen on the overall activity and product distribution observed in the conversion of 10 wt% methyl octanoate in methanol over the CsNaX catalyst. Table 3 summarizes the conversion and product distribution obtained on CsNaX at various reaction conditions.

Interestingly, very similar activity, stability (not shown) and product selectivity were observed at 425 °C when comparing the reaction under H_2 and under He. The main decarbonylation products, C7 and C6 olefins, were dominant under both gases, indicating little effect of gas-phase hydrogen in this reaction. It is also interesting to note that the octene yield obtained when using He was higher than when using H_2 as a carrier gas. This result demonstrates that the decarbonylation over CsNaX does not require gas-phase hydrogen when methanol is used as a solvent. The presence of hydrogen also had no effect on the catalyst stability, indicating that hydrogenation of carbonaceous residues does not take place.

To investigate the effect of reaction temperature, a run was conducted at 400 °C, rather than at 425 °C. As summarized in Table 3, the conversion decreased compared to the same reaction at 425 °C. The changes in selectivity are consistent with higher activation energies for the decarbonylation and deacetalation reactions compared to the rest, particularly the coupling reactions. That is, while the selectivity to hexene and heptene slightly decreases at 400 °C, the selectivity to the coupling products increased.

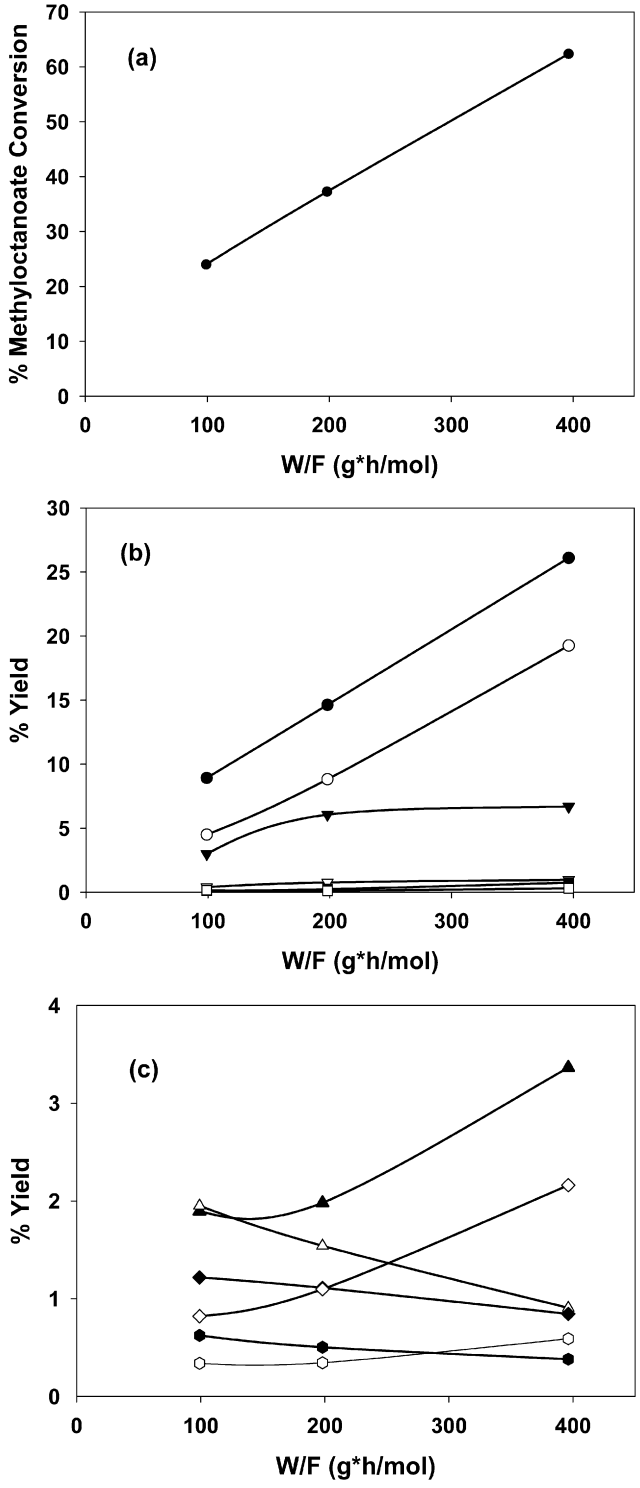

Fig. 8. Conversion (a), yields of major products (b), yields of minor products (c) from the reaction of 10 wt% methyl octanoate in methanol over CsNaX as a function of W/F. Reaction conditions: 425 °C, 1 atm, 25 ml/min of He. Heptenes (●), hexenes (○), octenes (▼), octane (▽), heptane (■), hexane (□), oxygenates (▲), pentadecanone (△), coupling ester (◆), octanoic acid (◇), octanal (⬢), tetradecene (○).

3.3.2. NaX and MgO catalysts

The deoxygenation activity of methyl octanoate over NaX and MgO catalysts were also studied and compared to that on CsNaX catalyst. Fig. 9 illustrates the product distribution obtained over NaX as a function of time on stream, keeping the same conditions as those used over CsNaX (compare with Fig. 7b). In significant contrast with the product distribution obtained on CsNaX, it

Table 3
Product distribution from reaction of 10 wt% methyl octanoate over CsNaX using methanol as solvent at various conditions

	Conditions		
Carrier gas	He	H_2	He
Reaction temperature (°C)	425	425	400
Conversion	37.2	34.8	10.8
Decabonylation/coupling ratio	11.4	8.3	5.0
Olefin/paraffin ratio	25.7	24.5	14.2
Selectivity (%)			
Hexenes	23.7	22.3	20.2
n-Hexane	0.3	0.9	1.8
Heptenes	39.4	40.7	35.8
n-Heptane	0.5	0.9	1.8
Octenes	16.4	10.9	9.2
n-Octane	2.2	1.4	0.9
Octanal	1.3	2.0	1.8
Oxygenates	5.4	6.6	8.3
Octanonic acid	3.0	3.4	3.7
Tetradecene	0.8	1.1	0.9
Pentadecanone	4.0	6.0	9.2
Coupling ester	3.0	3.7	6.4

Reaction conditions: $W/F = 198$ g h/mol.

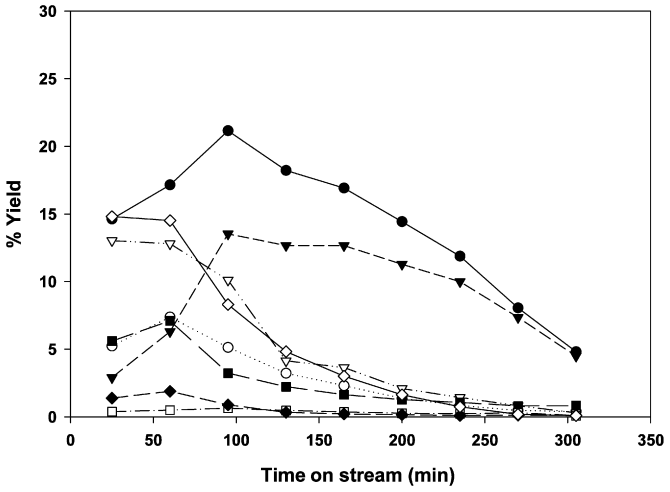

Fig. 9. Product distribution from the reaction of 10 wt% methyl octanoate in methanol over NaX zeolite catalyst as a function of time on stream. Reaction conditions: 425 °C, 1 atm, $W/F = 198$ g h/mol, 25 ml/min of He. Hexenes (●), heptenes (▼), multisubstituted aromatics (◇), heptane (▽), octenes (■), hexane (○), octane (□), and coupling hydrocarbons (◆).

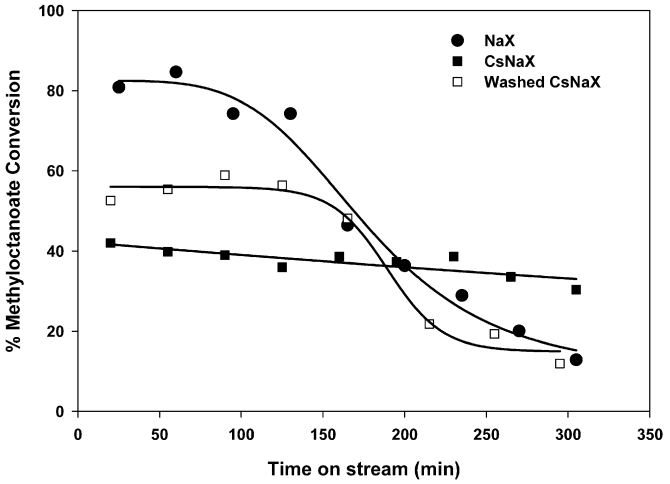

Fig. 10. Conversion of 10 wt% methyl octanoate in methanal over NaX as a function of time on stream, compared to that on CsNaX. Reaction conditions: 425 °C, 1 atm, $W/F = 198$ g h/mol, 25 ml/min of He.

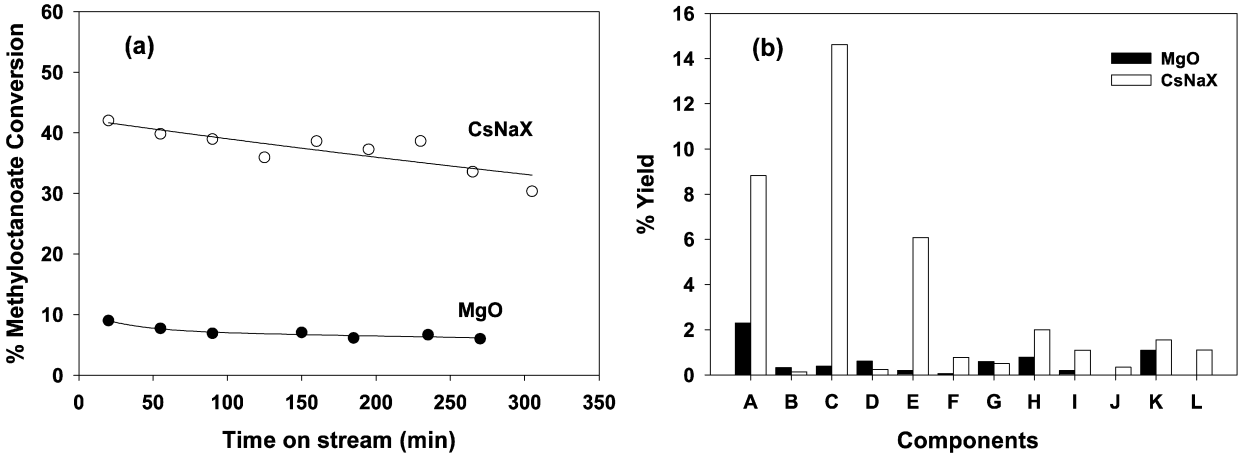

Fig. 11. Conversion (a) and product distributions (b) of 10 wt% methyl octanoate in methanol from the reaction over CsNaX and MgO catalysts. Reaction conditions: 425 °C, 1 atm, $W/F = 198$ g h/mol, 25 ml/min of He. (A) Hexenes, (B) hexane, (C) heptenes, (D) heptane, (E) octenes, (F) octane, (G) octanal, (H) oxygenates, (I) octanoic acid, (J) tetradecene, (K) pentadecanone, (L) coupling ester.

was observed that on this catalyst hexenes, heptenes, and multi-substituted aromatics were the dominant products at the beginning of the reaction. Then, as the catalyst deactivated, the aromatic products tended to disappear and only hexenes and heptenes were obtained as main products at longer time on stream. Moreover, on this catalyst, methanol conversion to dimethyl ether was observed to a significant extent, while absent on the Cs-containing catalyst. Both cyclization and etherification are reactions typically catalyzed by acids, which indicates that the NaX zeolite used in this study contains some acidity, in agreement with previous reports [32]. Also, typical of acid catalysts, rapid deactivation is observed with NaX (see Fig. 10). As shown below, this deactivation is probably due to coke formation over the acid sites, leading to a more rapid decrease in the production all the acid catalyzed products, namely multi-substituted aromatics, small alkanes, and dimethyl ether. It is interesting that as the acid sites become deactivated, decarbonylation can still proceed and deactivates at a lower rate, leading to a gradual decrease in hexenes and heptenes with time on stream. In line with this concept, the activity of washed CsNaX falls between that of CsNaX and that of NaX. Again, the additional (unselective) activity and more rapid deactivation, as compared to the unwashed CsNaX, can be related to the small amount of acid sites generated after the successive washing treatments.

To compare to a nonzeolitic basic catalyst, the reaction of 10% methyl octanoate in methanol was investigated under the same conditions as those used for the zeolite catalysts. The conversion and product distribution obtained over this catalyst are shown in Figs. 11a and 11b, respectively. It can be seen that a significantly lower conversion was obtained over MgO compared to that over CsNaX. In addition to differences in basicity, the lower catalytic activity of MgO can be attributed to its lower surface area (<40 m^2/g), as compared with that of the zeolites (>400 m^2/g). Moreover, MgO not only shows differences in the activity level, but also in selectivity, which is much lower towards the target hydrocarbon products and higher to undesired condensation products (such as 8-pentadecanone) compared to the high selectivity to C7–C8 hydrocarbons displayed by CsNaX.

3.4. Characterization of spent catalysts

The coke residues left on the catalysts after the conversion of methyl octanoate were quantified by TPO. Fig. 12 shows that when nonane was used as a solvent, more than twice as much coke was deposited on CsNaX as when methanol was used. This difference in coke deposition explains the different deactivation rates observed when nonane was used instead of methanol as a solvent. It can also be seen that the oxidation of the deposits from these reactions appeared at a relatively lower temperature (~280 °C), as compared to that of conventional hydrocarbon coke deposits (>550 °C). This suggests that the deposits on CsNaX are mainly high-molecular-weight oxygenates rather than the typical polynuclear aromatic coke.

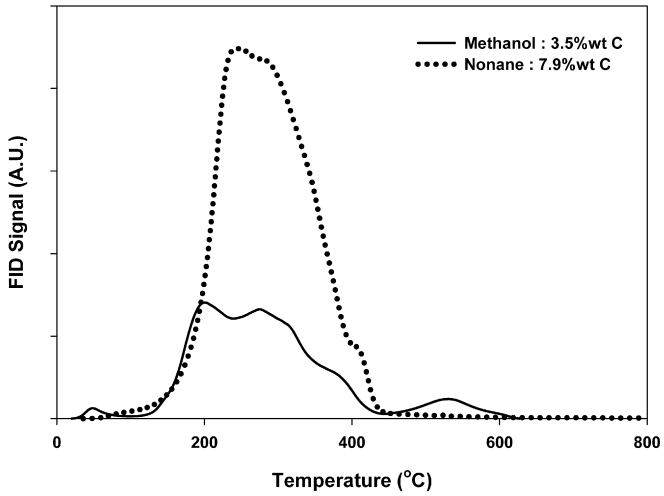

Fig. 12. TPO profiles of spent CsNaX catalysts from the reaction of 10 wt% methyl using nonane and methanol as solvent.

Fig. 13 shows the TPO profiles of the coke deposited during the reaction of 10% methyl octanoate in methanol over NaX, compared to CsNaX. It is clear that on NaX not only a significantly higher amount of deposits was formed, but also there is an important fraction of the deposits that decomposes at significantly higher temperature (350 °C), as compared with that in CsNaX. In line with the concepts discussed above, this additional deposit may be derived from the residues resulting from acid-catalyzed reactions. While the oxidation temperature of these species is higher than that observed with the basic CsNaX catalyst, it is much lower than that typically observed over strong acid catalysts. Hence, these deposits should not be referred to as polynuclear aromatic coke, but rather as oxygenated aromatic compounds formed over the weak acid sites of NaX.

4. Discussion

The rapid deactivation of the CsNaX zeolite catalyst observed during the reaction of methyl octanoate in nonane is presumably

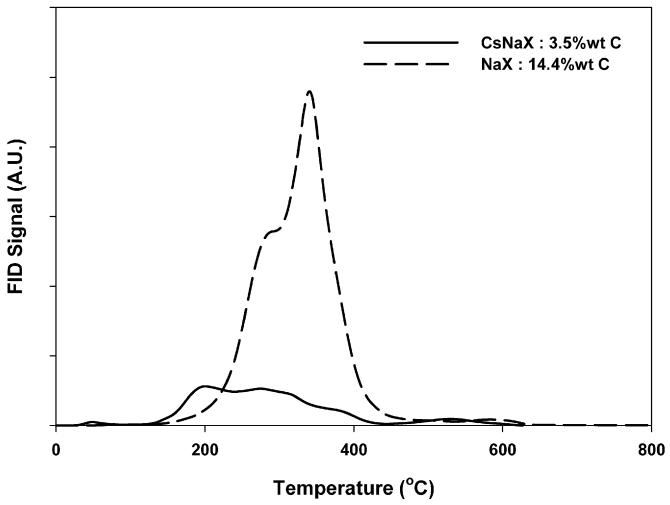

Fig. 13. TPO profiles of spent CsNaX and NaX catalysts from the reaction of 10 wt% methyl octanoate in methanol.

due to the adsorption of methyl octanoate on the highly basic sites of the zeolite that may not be greatly affected by the presence of the hydrocarbon solvent. Such strong adsorption may lead to a rapid deactivation by site (and probably pore) blockage. Under these conditions, the adsorbed methyl octanoate can react with each other (self-condensation) forming the observed high-molecular-weight oxygenates (e.g. 8-pentadecanone). Such compounds cannot readily diffuse out from the pores of the zeolite and lead to further blockage. The formation of high-molecular weight products is usually derived from (i) condensation (mostly aldol type) of the carbanion intermediates with available electrophilic species [33], or (ii) self-condensation [34]. It must be noted that these coupling products do not necessarily form a hard coke, since, as the TPO results show, they can be removed at relatively low oxidation temperatures (i.e. below 300 °C).

By contrast, the use of methanol as a solvent generates a completely different situation. First, the catalytic stability of CsNaX is greatly enhanced. Methanol being a highly polar molecule, it can competitively interact with the zeolite basic sites [18]. Several reports [35,36] have suggested that adsorption of methanol derives mainly from interactions between the methoxyl oxygen and the exchangeable cation and interactions between the hydroxyl hydrogen and the framework oxygen:

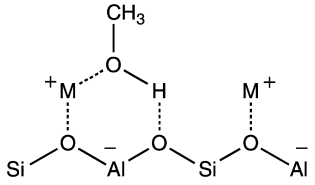

When M^+ is Cs^+, a highly polarizable cation, the interaction between M^+–O is relatively weaker than that with higher Lewis acid Na^+. However, over CsNaX, the framework O–H interaction becomes stronger and hence this weakens the O–H of methanol. As shown in the TPD and TPRx studies, this interaction leads to the decomposition of methanol to yield primarily a surface CH_2O and hydrogen. The surface CH_2O would then form a formate-like species, which can be further converted into a carbonate-like species as the temperature increases, as evidenced by NMR signals at 166 and 171 ppm, respectively [30].

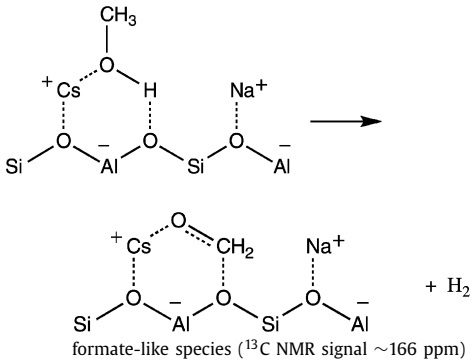

formate-like species (^{13}C NMR signal ~166 ppm)

Under our reaction conditions, we expect that both surface formate and surface carbonate species will be present. These species can readily compete with the adsorption of methyl octanoate, thus lowering its surface coverage and inhibiting the self-condensation reaction. As a result, this adsorption inhibition suppresses the formation of high-molecular weight oxygenates, resulting in better catalytic stability. Also, consistent with the above discussion, a lower initial activity can be expected for the reaction in the presence of methanol, as experimentally observed. Since there is no significant difference in activity and product selectivity when hydrogen is used as carrier gas, we may suggest that the hydrogen, produced in situ from the methanol decomposition, can further facilitate the hydrogenation of methyl octanoate and its primary products. Hence, various olefins and alkanes, such as octene, hexane and heptane were obtained from the reaction using methanol as a solvent.

As suggested by TPD results (Fig. 5), the methyl octanoate is strongly adsorbed on basic sites of CsNaX. Due to the highly polarizable nature of methyl octanoate, the interaction between carbonyl ester and the basic framework oxygen would readily weaken the carboxylate C–O bond, leading to the decomposition of the ester into two surface-aldehydes, as generally observed over typical basic catalysts [37]. In this case, the decomposed methoxyl group would form the formate-like species (surface-formaldehyde) while the other fragment would form an "octanoate-like species" (surface-octanaldehyde), in parallel with the formation of the formate-like species discussed above. This formate-like species would then decompose into carbon monoxide and hydrogen, in a manner similar to that observed with methanol. This primary decomposition of the methoxyl group is evidenced in the present study by the observed CO evolution prior to the formation of hydrocarbon (~300–400 °C). The fact that the amount of CO evolved at this temperature range (~1.6 μmol/g) is relatively small compared to that evolved at higher temperatures (~6.8 μmol/g), suggests that the decomposition of the formate-like species was not the dominant path, but the species was retained on the surface up to higher temperatures.

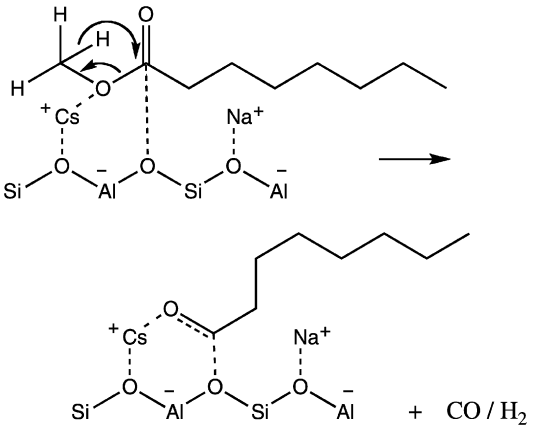

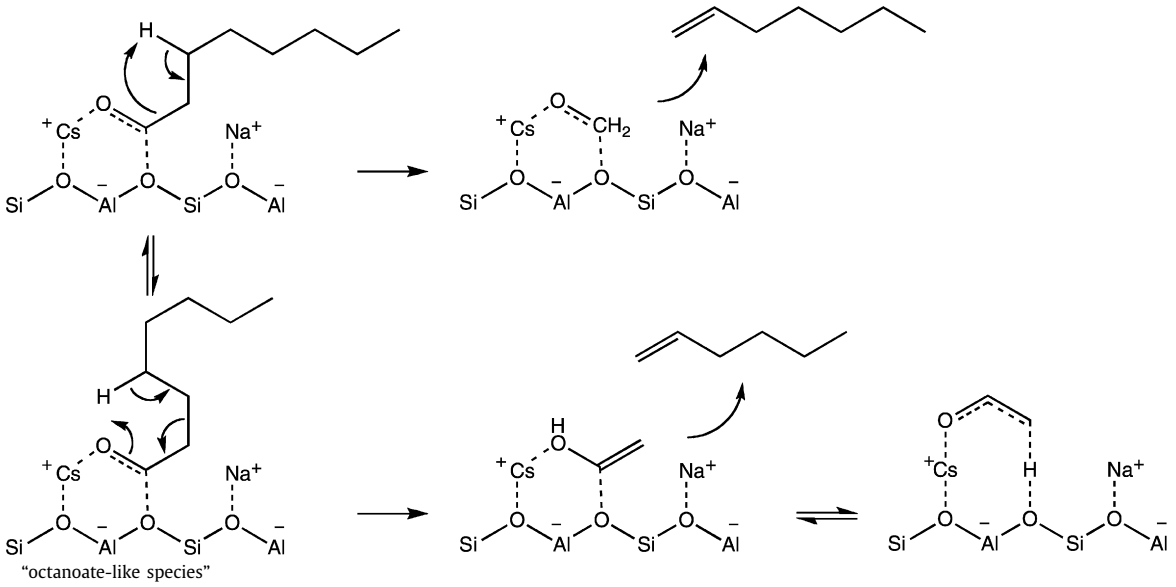

Chart 1

It is proposed that decomposition of such "octanoate-like species" leads to the formation of the two major hydrocarbon products observed on the CsNaX catalyst, heptene and hexene (see Chart 1). In the first case, the well-known β-hydrogen elimination [38] and subsequent decomposition would result in heptene as major product of the reaction, with parallel evolution of CO and H_2. This reaction may well be referred to as a reversible reaction of the typical hydroformylation [39]. In the second case, the decomposition of a cyclic-like intermediate can lead to the formation of more electrophilic acetaldehyde (enol-form) and hexene, as shown. The acetaldehyde may be evolved as a by-product or may undergo further aldol condensation/alkylation to form C3–C5 oxygenates, as observed in small amounts by GC-MS.

It must be noted that while hydrogen is not required for the production of heptenes and hexenes it is necessary for the formation of octenes and alkanes via hydrogenation/dehydration. These reactions can indeed occur on cesium-exchanged zeolites [40]. As discussed above, due to the highly polarizable cesium cations, the basic sites associated with it can readily decompose the methanol/methoxyl group, creating a hydrogen surface fugacity well above that in equilibrium with hydrogen in the gas phase [41,42]. With such high virtual pressure of hydrogen, the adsorbed "octanoate-like species" may well be hydrogenated forming primarily an octanol that then rapidly undergoes dehydration to form octenes:

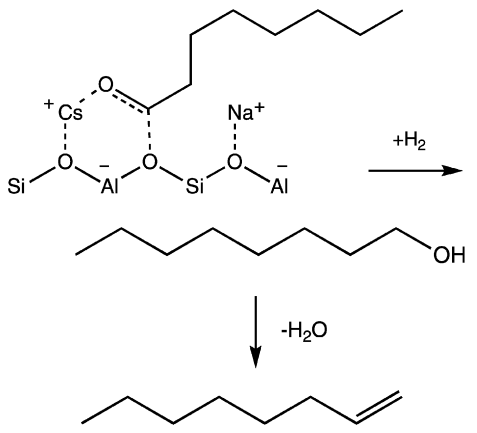

The small amounts of octane, heptane and hexane in the product give evidence for the hydrogenation activity of CsNaX (see Table 2). However, the extent of this reaction is small in comparison to that of the octanoate-like species decomposition. This is because olefins are less adsorptive on the basic sites, as compared to the more electrophilic octanoate-like species. These hydrogenolysed/hydrogenated products can be particularly promoted in the reaction with methanol, but not readily with nonane (Fig. 7).

The observed small amounts of 8-pentadecanone and long-chain olefins suggest another reaction path on CsNaX. We believe that 8-pentadecanone is not derived from the "octanoate-like" intermediate responsible for the production of heptenes and hexene. Instead, this large product is likely to arise from the decomposition of an acid anhydride. The adsorbed methyl octanoate may undergo a condensation reaction, forming dioctanoic acid anhydride. The acid anhydride may undergo a decarboxylation to ketone [43] on the basic sites since the highly negative framework charge of oxygen would act as an acceptor for the acidic CO_2. This path would explain the high yield of 8-pentadecanone observed in the reaction when nonane is used as a solvent.

Due to its low mobility, 8-pentadecanone is likely to stay on surface long enough to be hydrogenated by the adsorbed H to form alcohol, but such a heavy alcohol would undergo dehydration, forming a long-chain inner olefin. In fact, as W/F increases, 8-pentadecanone is seen to be readily converted and this is consistent with the observed increase in the yields of long-chain olefins at longer space times.

The comparison of the catalytic behavior of CsNaX with those of NaX and MgO indicates that the presence of polarizable Cs cations result in a catalyst with unique performance. First, on the latter catalysts, the decarbonylation/deacetalation activity is not as pronounced as over CsNaX. Also, since the Na cation is much harder than the Cs cation [44] it holds the negative framework charge more tightly and thus it provides less Lewis basicity to the framework oxygen [45]. That is, the presence of Na as exchangeable cation, leads to an increase in the (weak) acidity of the Lewis sites in the zeolite, as evidenced by IPA-TPD. This weak acidity would explain the formation of aromatic products and the rapid deactivation over NaX. Consistent with this view, a higher amount of coke deposits was found on NaX, with an important fraction of the carbonaceous species decomposed at relatively high temperature (Fig. 13).

It should be noted that the yield of hexene is higher than that of heptene over NaX, but the opposite is true for CsNaX. This difference suggests that in the case of NaX additional hexenes are produced by cracking of higher molecular weight compounds, not only from the deacetalation that occurs in CsNaX. The additional yields due to cracking would also be applied to heptene and other hydrocarbons formed, and hence these reactions give a higher initial conversion over this catalyst. It is also interesting to note that, after the weak acid sites are deactivated in NaX, the production of heptene and hexene slowly decreases with time on stream (Fig. 9). As proposed above, these products arise from both cracking over acid sites and by decarbonylation/deacetalation over basic sites. As the acid sites are deactivated while the latter are still active, a gradual decrease only in these two products with time on stream is observed. Accordingly, since after about 250 min on stream the acid function has been completely eliminated, the residual activity can be ascribed to the decarbonylation/deacetalation activity of NaX.

The suggestion that the alkali-exchanged zeolites contain both acid and basic functions, is in agreement with earlier studies [46,47] which indicate that NaX can be regarded as an amphoteric catalyst, interacting with polar oxygenates in a manner totally different from that observed over CsNaX. For example, over NaX, methanol competes with methyl octanoate for adsorption and consequently DME is largely produced by dehydration of methanol. Also, on this catalyst, in addition to decarbonylation, methyl octanoate undergoes acid-catalyzed reactions, such as cracking, isomerization, alkylation, dimerization, and even aromatization. Hence, multi-substituted aromatics are obtained over NaX since methanol can readily act as a methylating agent over weakly acidic sites. When the acid sites are deactivated, the cracking products and aromatics virtually disappear. Only decarbonylation and deacetalation activity due to negative framework charge of NaX remains. However, this is to a much lower extent than on CsNaX. In addition, it can be seen that on NaX, without Cs, no hydrogenation activity can be observed and the use of methanol as a solvent does not facilitate the maintenance of the desirable reactions.

Finally, by analyzing the behavior observed on the MgO catalyst, one can conclude that not only the basicity is required for decarbonylation, but also the highly polar environment of the zeolite micropore seems to play an essential role in adsorption and decomposition of the adsorbed species. Although MgO is well regarded as a highly basic catalyst, its two-dimensional surface cannot readily facilitate the adsorption and decomposition of methyl octanoate. In addition, a much lower surface area, as compared to that of the zeolites, would show a significant effect on activity. Hence, on this catalyst only small amounts of deoxygenate products were obtained, as compared to that on CsNaX. By contrast, the MgO catalyst seems to display enough basicity to activate the coupling reaction of methyl octanoate, thus resulting in the formation of 8-pentadecanone. As mentioned above, the 8-pentadecanone is formed via the decomposition of an acid anhydride intermediate. As the acid anhydride is a “hard” species, it would possess a better interaction and decomposition to 8-pentadecanone over the “hard” MgO base.

While MgO can readily decompose methanol to CO and H_2 [48], only small amounts of octene and hydrogenated products can be found over this catalyst. It is believed that the absence of highly polarisable cesium cations and the absence of the highly polar environment in the restricted pores of the zeolites limit the ability of MgO to adsorb and dissociate hydrogen which results in lower surface fugacity of hydrogen than in the case of the zeolites. Therefore, hydrogenation cannot be readily promoted on MgO and yields of octene, heptane and hexane are relatively small.

5. Conclusions

It can be concluded that the decarbonylation/deacetalation activity of methyl octanoate can occur at high rate and for a long time on stream over CsNaX catalyst when co-feeding methanol. Methyl octanoate strongly adsorbs on CsNaX basic sites and cannot be desorbed unless decomposed. When a weak adsorbent as nonane is co-fed CsNaX rapidly deactivates. By contrast, when methanol is co-fed with methyl octanoate, the catalyst stability is greatly enhanced due to the presence of decomposed fragments of methanol on the surface. These fragments are formate-like species that prevent self-condensation and formation of higher molecular weight oxygenates. The TPD results suggest that the decarbonylation of methyl octanoate proceeds via primary decomposition at the methoxyl group, presumably producing an octanoate-like species as intermediate. The direct decomposition of this species gives heptenes and hexenes as main products. Octenes and other hydrogenated products are formed by hydrogenation/dehydration, in which the surface hydrogen produced from methanol decomposition plays an important role.

When Cs is not present (NaX zeolite) the catalyst basicity is much lower and the weak acid sites dominate the behavior of the catalyst. The net results are a decrease in the decarbonylation/deacetalation activity, together with an increase in the selectivity toward undesired products. The poor performance displayed by the MgO catalyst indicates that not only the basicity is required for decarbonylation, but also the highly polar environment characteristic of the zeolite micropore seems to play an essential role.

In summary, the use of the basic characteristics of Cs cation exchanged in zeolite X and methanol as a co-reactant appears as an effective combination for the conversion of methyl-esters to hydrocarbons, a reaction that may have practical application in the refining of biodiesel with low hydrogen consumption.

Acknowledgments

This work was financially supported by the Oklahoma Secretary of Energy and the Oklahoma Bioenergy Center. The authors would like to thank Mr. Surapas Sitthisa for TPR and TPO analysis. One of the authors (T.S.) thanks the Fulbright Thai visiting program for support, and (T.D.) thanks the Thailand Research Fund for a scholarship.

References

[1] D.E. Lopez, K. Suwannakarn, D.A. Bruce, J.G. Goodwin Jr., J. Catal. 247 (2007) 43.
[2] I.N. Martyanov, A. Sayari, Appl. Catal. A 339 (2008) 45.
[3] D.A.G. Aranda, R.T.P. Santos, N.C.O. Tanpanes, A.L.D. Ramos, O.A.C. Antunes, Catal. Lett. 122 (2008) 20.
[4] M.D. Serio, R. Tesser, L. Pengmei, E. Santacesaria, Energy Fuels 22 (2008) 207.
[5] G. Knothe, Fuel Process. Technol. 86 (2005) 1059.
[6] G. Knothe, A.C. Matheaus, T.W. Ryan III, Fuel 82 (2003) 971.
[7] G. Knothe, Fuel Process. Technol. 88 (2007) 669.
[8] W.F. Maier, P. Grubmiller, I. Thies, P.M. Stein, M.A. McKervey, P.R. Schleyer, Angew. Chem. Int. Ed. 18 (2003) 939.
[9] D.S. Brands, G. U-A-Sai, E.K. Poels, A. Bliek, J. Catal. 186 (1999) 169.
[10] T.A. Foglia, P.A. Barr, J. Am. Oil Chem. Soc. 53 (1976) 737.
[11] I. Kubickova, M. Snare, K. Eranen, P. Maki-Arvela, D.Y. Murzin, Catal. Today 106 (2005) 197.
[12] P. Maki-Arvela, I. Kubickova, M. Snare, K. Eranen, D.Y. Murzin, Energy Fuels 21 (2007) 30.
[13] M. Snare, I. Kubickova, P. Maki-Arvela, K. Eranen, J. Warna, D.Y. Murzin, Chem. Eng. J. 134 (2007) 29.
[14] G.N. Rochafilho, D. Brodzki, G. Djega-Mariadassou, Fuel 72 (1993) 543.
[15] M. Snare, I. Kubickova, P. Maki-Arvela, D. Chichova, K. Eranen, D.Y. Murzin, Fuel 87 (2008) 933.
[16] I. Rodriguez, H. Cambon, D. Brunel, M. Lasperas, J. Mol. Catal. A Chem. 130 (1998) 195.
[17] X.F. Zhang, E.S.M. Lai, R. Martin-Aranda, K.L. Yeung, Appl. Catal. A Gen. 261 (2004) 109.

[18] T. Sooknoi, J. Dwyer, J. Mol. Catal. A Chem. 211 (2004) 155.
[19] P. Belirame, P. Fumagallip, G. Zuretti, Ind. Eng. Chem. Res. 32 (1993) 26.
[20] D. Barthomeuf, Catal. Rev. 38 (1996) 521.
[21] M. Lasperas, H. Cambon, D. Brunel, I. Rodriguez, P. Geneste, Microporous Mater. 7 (1996) 61.
[22] M. Lasperas, H. Cambon, D. Brunel, I. Rodriguez, P. Geneste, Microporous Mater. 1 (1993) 343.
[23] P.E. Hathaway, M.E. Davis, J. Catal. 116 (1989) 263.
[24] Y. Sun, Z. Liu, P. Pianetta, D. Lee, J. Appl. Phys. 102 (2007) 074908.
[25] E.A. Podgornov, I.P. Prosvirin, V.I. Bukhtiyarov, J. Mol. Catal. A Chem. 158 (2008) 337.
[26] R. Schenkel, A. Jentys, S.F. Parker, J.A. Lercher, J. Phys. Chem. B 108 (2004) 7902.
[27] N. Takahashi, A. Mijin, T. Ishikawa, K. Nebuka, H. Suematsu, J. Chem. Soc. Faraday Trans. I 83 (1987) 2605.
[28] F. Yagi, H. Tsuji, H. Hattori, Microporous Mater. 9 (1997) 237.
[29] S. Imamura, T. Higashihara, Y. Saito, H. Aritani, H. Kanai, Y. Matsumura, N. Tsuda, Catal. Today 50 (1999) 369.
[30] M. Hunger, U. Schenk, M. Seiler, J. Weitkamp, J. Mol. Catal. A Chem. 156 (2000) 153.
[31] G.W. Huber, A. Corma, Angew. Chem. Int. Ed. 46 (2007) 7184.
[32] H.B. Schwarz, S. Ernst, J. Karger, B. Knorr, G. Seiffert, R.Q. Snurr, B. Staudte, J. Weitkamp, J. Catal. 167 (1997) 248.
[33] J. Li, J. Tai, R.J. Davis, Catal. Today 116 (2006) 226.
[34] N.D. Plint, N.J. Coville, D. Lack, G.L. Nattrass, T. Vallay, J. Mol. Catal. A Chem. 165 (2001) 275.
[35] D.F. Plant, A. Simperler, R.G. Bell, J. Phys. Chem. B 110 (2006) 6170.
[36] P. Mignon, P. Geerling, R. Schoonheydt, J. Phys. Chem. B 110 (2006) 24947.
[37] H.N. Wright Jr., H.J. Hagemeyer Jr., US Patent 3,714,236 (1973).
[38] N. Takahashi, H. Matsuo, M. Kobayashi, J. Chem. Soc., Faraday Trans. 1 80 (1984) 629.
[39] G. Cuma, P. Famulari, M. Marchetti, B. Sechi, J. Mol. Catal. A Chem. 218 (2004) 211.
[40] T. Sooknoi, J. Dwyer, Stud. Surf. Sci. Catal. 97 (1995) 423.
[41] E. Iglesia, J.E. Baumgartner, G.L. Price, J. Catal. 134 (1992) 549.
[42] M. Boudart, Catal. Lett. 3 (1989) 111.
[43] M. Glinski, W. Szymanski, D. Lomot, Appl. Catal. A 281 (2005) 107.
[44] R.G. Pearson, J. Am. Chem. Soc. 85 (1963) 3533.
[45] Y. Okamato, M. Ogawa, A. Maezawa, T. Imanaka, J. Catal. 112 (1988) 427.
[46] F. Horst, F. Hartmut, G. Ekkehard, H. Bernd, J. Herve, K. Christine, K. Olaf, K. Knut, Phys. Chem. Chem. Phys. 1 (1999) 593.
[47] J.A. Lercher, A. Jentys, A. Brait, Mol. Sieves Sci. Technol. 6 (2008) 153.
[48] D.C. Foyt, J.M. White, J. Catal. 47 (1977) 260.